Improved bounds on the effective conductivity of high-contrast suspensions

S. Torquato[a)]
Courant Institute of Mathematical Sciences, New York University, 251 Mercer Street, New York, New York 10012

J. Rubinstein
Department of Mathematics, Technion-Israel Institute of Technology, 32000 Haifa, Israel

(Received 10 December 1990; accepted for publication 15 February 1991)

Conventional upper and lower bounds on the effective conductivity σ_e of two-phase composite media diverge from one another in the infinite-contrast limits ($\alpha = \infty$ or 0). We have derived a generally nontrivial upper bound on σ_e for suspensions of identical spheres when the spheres are superconducting, i.e., the upper bound does not necessarily become infinite in the limit $\alpha \to \infty$. Similarly, a generally nontrivial lower bound on σ_e is derived for the aforementioned suspension when the spheres are perfect insulators, i.e., the lower bound does not necessarily vanish in the limit $\alpha \to 0$. The bounds are computed for two models: simple cubic arrays and random arrays of spheres.

I. INTRODUCTION

Virtually all previously derived rigorous upper and lower bounds on the effective conductivity σ_e of two-phase composites, such as the well-known Hashin–Shtrikman[1] and higher-order Beran[2] and Milton[3] bounds, diverge from one another in the limits of infinite contrast ($\alpha = \infty$ and 0). For example, such conventional upper bounds tend to infinity when $\alpha = \sigma_2/\sigma_1 \to \infty$ and lower bounds vanish in the limit $\alpha \to 0$, where σ_i is the conductivity of phase i. The corresponding reciprocal bounds in each of these instances (i.e., lower bounds when $\alpha = \infty$ and upper bounds when $\alpha = 0$) remain finite and, as noted by Torquato,[4] can still yield good estimates of the effective conductivity, depending on whether the system is below or above the percolation threshold. This observation has been borne out by recent computer-simulation experiments for the effective conductivity.[5] Thus, the aim of this paper is to begin a program to improve upon conventional upper bounds when phase 2 is superconducting relative to phase 1 ($\alpha = \infty$) and conventional lower bounds when phase 2 is perfectly insulating relative to phase 1 ($\alpha = 0$).

The aforementioned bounds apply to general isotropic media and incorporate limited statistical information on the composite. The upper bounds go to infinity when $\alpha \to \infty$ because they take into account realizations in which phase 2 is continuously connected, even if phase 2 is disconnected in the actual microgeometry. Similarly, conventional lower bounds vanish when $\alpha \to 0$ because they take into account realizations in which phase 1 is continuously connected. Therefore, in order to avoid such behavior, one must devise bounds which contain specific information prohibiting connected realization from occurring when the relevant phase is below its percolation threshold. One way of accomplishing this for the case of suspensions of identical spheres, the geometry focused on in this study, is by employing "security-spheres" trial fields in variational principles. Keller, Rubenfeld, and Molyneux[6] were the first to use the security-spheres approach to derive bounds on the effective viscosity of a suspension. Security-spheres bounds were subsequently derived for the trapping constant[7] and fluid permeability[8] of porous media. Security-spheres conductivity bounds have heretofore not been formulated.

The purpose of this paper is to derive security-sphere bounds for the effective conductivity of high-contrast suspensions of identical spheres. It will be shown that the security-spheres upper bound (in contrast to the Hashin–Shtrikman upper bound, for example) does not necessarily become infinite in the limit of superconducting spheres ($\alpha = \infty$). Similarly, the security-spheres lower bound does not necessarily vanish in the limit of perfectly insulating spheres ($\alpha = 0$).

We recently learned of bounds on σ_e derived by Bruno[9] which, in the spirit of the security-spheres bounds developed in the present study, give nontrivial bounds in the infinite-contrast limits. For reasons described in Sec. III, his upper bound for $\alpha = \infty$ and lower bound for $\alpha = 0$ are sharper than the corresponding security-spheres bounds when the particles are "well spaced from one another," such as in a periodic array of spheres. On the other hand, the same security-spheres bounds can be appreciably sharper than Bruno's corresponding bounds when the particles are not well spaced from one another, such as random arrays of spheres over a wide volume-fraction range. By the phrase "well spaced from one another" we mean that the fluctuations in the mean nearest-neighbor distances between particles are small. Henceforth, we will simply refer to such an array as "well spaced." Note that by this definition, a periodic array at close packing is well spaced.

[a)]On leave of absence from the Department of Mechanical and Aerospace Engineering, North Carolina State University, Raleigh, NC 27695-7910 until 31 May 1990.

 0021-8979/91/107118-08$03.00

II. NEW CONDUCTIVITY BOUNDS

A. General variational principles

The random medium is generally a domain of space $V(\omega)\in\Re^3$ (where the realization ω is taken from some probability space Ω) of volume V, which is composed of two regions: the phase-1 region V_1 of volume fraction ϕ_1 and conductivity V_1 and the phase-2 region V_2 of volume fraction ϕ_2 and conductivity σ_2. The characteristic function of phase i is defined by

$$I^{(i)}(\mathbf{x})=\begin{cases}1, & \mathbf{x}\in V_i(\omega),\\ 0 & \text{otherwise.}\end{cases} \tag{1}$$

Thus, the local conductivity $\sigma(\mathbf{x})$ is given by

$$\sigma(\mathbf{x})=\sigma_1 I^{(1)}(\mathbf{x})+\sigma_2 I^{(2)}(\mathbf{x}). \tag{2}$$

For macroscopically isotropic two-phase media with effective conductivity σ_e, we shall make use of two variational principles: minimum potential energy and minimum complementary potential energy.[2,10]

1. Minimum potential energy

The effective conductivity is bounded from above according to the following relation:

$$\sigma_e\leqslant\frac{\langle\sigma\hat{\mathbf{E}}\cdot\hat{\mathbf{E}}\rangle}{\langle\mathbf{E}\rangle\cdot\langle\mathbf{E}\rangle},\quad \forall\hat{\mathbf{E}}\in A, \tag{3}$$

$$A=\{\hat{\mathbf{E}};\nabla\times\hat{\mathbf{E}}=0\text{ in }\Re^3,\langle\hat{\mathbf{E}}\rangle=\langle\mathbf{E}\rangle\}. \tag{4}$$

Here A is the class of admissible or trial gradient fields $\hat{\mathbf{E}}$. The quantity $\hat{\mathbf{E}}$ is the actual field which for the electrical and thermal problems represent the electric field and the negative of the temperature gradient, respectively. Angular brackets denote an ensemble average. The irrotational condition in (4) implies the existence of a potential which must be continuous across the two-phase interface.

2. Minimum complementary potential energy

The effective conductivity is bounded from below according to the following expression:

$$\sigma_e\geqslant\frac{\langle\mathbf{J}\rangle\cdot\langle\mathbf{J}\rangle}{\langle\sigma^{-1}\hat{\mathbf{J}}\cdot\hat{\mathbf{J}}\rangle},\quad \forall\hat{\mathbf{J}}\in B, \tag{5}$$

$$B=\{\hat{\mathbf{J}};\nabla\cdot\hat{\mathbf{J}}=0\text{ in }\Re^3,\langle\hat{\mathbf{J}}\rangle=\langle\mathbf{J}\rangle\}. \tag{6}$$

Here, B is the class of admissible or trial flux fields $\hat{\mathbf{J}}$. The quantity $\mathbf{J}$ is the actual flux field which for the electrical and thermal problems represent the electrical current and heat flux, respectively. The solenoidal condition of (6) implies that the normal flux must be continuous across the two-phase interface.

In what follows, we shall invoke the ergodic hypothesis and thus will equate the ensemble average of a function f with the volume average in the infinite-volume limit, i.e.,

$$\langle f\rangle=\lim_{V\to\infty}\frac{1}{V}\int_V f\,dV. \tag{7}$$

B. Security-spheres upper bound

Consider constructing a trial gradient field $\hat{\mathbf{E}}$ for a distribution of N identical spheres of radius a of conductivity σ_2 in a matrix of conductivity σ_1. Let the distance between the ith sphere and its nearest neighbor be denoted by $2b_i$ such that $b_i>a$, $\forall i$. A trial field $\hat{\mathbf{E}}\in A$ [where A is given by (4)] is chosen as follows: For every sphere i centered at position $\mathbf{r}_i$ we consider the domain composed of the sphere and a concentric "security" sphere of radius b_i. In that domain we solve

$$\Delta u_i(\mathbf{x})=0,\quad \text{for } 0<|\mathbf{x}-\mathbf{r}_i|<b_i, \tag{8}$$

$$u_i \text{ finite at } |\mathbf{x}-\mathbf{r}_i|=0, \tag{9}$$

$$u_i \text{ and } U_n^{(i)} \text{ continuous at } |\mathbf{x}-\mathbf{r}_i|=a, \tag{10}$$

$$u_i=-|\mathbf{E}_0|b\cos\theta_i \text{ at } |\mathbf{x}-\mathbf{r}_i|=b_i. \tag{11}$$

Here, Δ is the Laplacian operator, $U_n^{(i)}$ is the normal flux associated with the potential u_i, θ is the polar angle associated with the radial distance $|\mathbf{x}-\mathbf{r}_i|$, and $\mathbf{E}_0$ is applied field equal to the actual average field $\langle\mathbf{E}\rangle$. The trial field $\hat{\mathbf{E}}$ is chosen so that

$$\hat{\mathbf{E}}(\mathbf{x})=-\nabla u_i, \tag{12}$$

in the security sphere, and

$$\hat{\mathbf{E}}(\mathbf{x})=\mathbf{E}_0(\mathbf{x}), \tag{13}$$

exterior to the security spheres.

The solution of the boundary-value problem (8)–(11) is given in Appendix A. Using this solution and (13), it is straightforward to show that

$$\frac{1}{V}\int_{V_O}\sigma\hat{\mathbf{E}}\cdot\hat{\mathbf{E}}\,dV=\frac{V_O}{V}\sigma_1\mathbf{E}_0\cdot\mathbf{E}_0 =\left(1-\phi_2\frac{1}{N}\sum_{i=1}^{N}\lambda_i^3\right)\sigma_1 E_0^2, \tag{14}$$

where

$$\phi_2=\frac{\rho 4\pi a^3}{3} \tag{15}$$

is the volume fraction of the spheres of radius a (with $\rho=N/V$ being the number density) and V_O is the volume exterior to the security spheres. Similarly, letting V_S denote the space interior to the security spheres, we have

$$\frac{1}{V}\int_{V_S}\sigma\hat{\mathbf{E}}\cdot\hat{\mathbf{E}}\,dV=\phi_2\frac{1}{N}\sum_{i=1}^{N}h(\lambda_i), \tag{16}$$

where

$$h(\lambda)=\frac{9\sigma_2\lambda^6+\sigma_1[(\alpha+2)^2\lambda^6+2(\alpha-1)^2\lambda^3](\lambda^3-1)}{[(\alpha+2)\lambda^3+(1-\alpha)]^2}, \tag{17}$$

$$\alpha=\frac{\sigma_2}{\sigma_1}. \tag{18}$$

Combination of the variational bound (3) and relations (14), (16), and (17) finally yields the security-spheres upper bound:

$$\frac{\sigma_e}{\sigma_1} \leqslant 1 + \phi_2 \frac{1}{N} \sum_{i=1}^{N} f(\lambda_i, \alpha), \tag{19}$$

where

$$f(\lambda,\alpha) = \frac{3(\alpha+2)(\alpha-1)\lambda^6 - 3(\alpha-1)^2\lambda^3}{[(\alpha+2)\lambda^3 + (1-\alpha)]^2}. \tag{20}$$

Since our primary interest will be in cases in which the contrast is infinite ($\alpha = \infty$ or 0), it is useful to note that

$$f(\lambda,\infty) = \frac{3\lambda^3}{\lambda^3 - 1}, \tag{21}$$

$$f(\lambda,0) = \frac{-3\lambda^3}{2\lambda^3 + 1}. \tag{22}$$

Using the law of large numbers, we have from (19) that

$$\frac{\sigma_e}{\sigma_1} \leqslant 1 + \phi_2 d \int_1^\infty f(x,\alpha) H(x) dx, \tag{23}$$

where H is the nearest-neighbor distribution function and $d = 2a$ is just the sphere diameter. The quantity $H(r)dr$ is the probability that, given any sphere of diameter d at the origin, the center of the nearest neighbor lies at a distance between r and $r + dr$. In (23), $x = r/d$ is a dimensionless distance. The nearest-neighbor distribution function $H(r)$ has recently been computed by Torquato, Lu, and Rubinstein[11] for random distribution of hard spheres to all orders of ϕ_2. Note that $H(r)$ has dimensions of inverse length.

The function $f(x,\alpha)$ has a simple pole at $x = 1$ for superconducting spheres ($\alpha = \infty$). Thus, the upper bound (23) remains finite when $\alpha = \infty$ provided that $H(x)$ vanishes as $(x-1)^\beta$ at $x = 1$, where $\beta > 0$. (In the subsequent section, we shall consider microgeometries for which the upper bound remains finite when $\alpha \to \infty$.) This behavior for $\alpha = \infty$ is to be contrasted with conventional bounds,[1-3] such as the well-known Hashin–Shtrikman[3] upper bound:

$$\left(\frac{\sigma_e}{\sigma_1}\right)_{\mathrm{HS}} = \frac{\alpha[1 + 2\phi_1(1-\alpha)/(1+2\alpha)]}{1 - \phi_1(1-\alpha)/(1+2\alpha)}, \tag{24}$$

which always diverges to infinity as $\alpha \to \infty$.

C. Security-spheres lower bound

We now consider constructing a trial flux field $\hat{\mathbf{J}}$ for a distribution of N identical spheres of radius a of conductivity σ_2 in a matrix of conductivity σ_1. Again, $2b_i$ is the distance between the ith sphere and its nearest neighbor. A trial field $\hat{\mathbf{J}} \in B$ [where B is given by (6)] is chosen as follows: For every sphere i centered at position $\mathbf{r}_i$, we consider the domain composed of the sphere and a concentric security sphere of radius b_i. In that domain we solve

$$\Delta v_i(\mathbf{x}) = 0, \quad \text{for } 0 \leqslant |\mathbf{x} - \mathbf{r}_i| \leqslant b_i, \tag{25}$$

$$v_i \text{ finite at } |\mathbf{x} - \mathbf{r}_i| = 0, \tag{26}$$

$$v_i \text{ and } V_n^{(i)} \text{ continuous at } |\mathbf{x} - \mathbf{r}_i| = a, \tag{27}$$

$$\frac{\partial v_i}{\partial y_i} = -|\mathbf{E}_0| \cos\theta \text{ at } |\mathbf{x} - \mathbf{r}_i| b. \tag{28}$$

Here, $V_n^{(i)}$ is the normal flux associated with the trial potential v_i and $y_i \equiv |\mathbf{x} - \mathbf{r}_i|$. Summation notation is not implied in (28). The trial flux $\hat{\mathbf{J}}$ is chosen such that

$$\hat{\mathbf{J}} = \begin{cases} -\sigma_2 \nabla v_i, & 0 \leqslant |\mathbf{x} - \mathbf{r}_i| < a, \\ -\sigma_1 \nabla v_i, & a \leqslant |\mathbf{x} - \mathbf{r}_i| \leqslant b_i, \end{cases} \tag{29}$$

in ith security sphere, and

$$\hat{\mathbf{J}} = \sigma_1 \mathbf{E}_0, \tag{30}$$

exterior to the security spheres.

The solution of the boundary-value problem (25)–(28) is given in Appendix B. Employing this solution and (30), it is easily shown (by the same methods of Sec. II B) that inequality (5) yields

$$\frac{\sigma_e}{\sigma_1} \geqslant \left(1 + \phi_2 d \int_1^\infty g(x,\alpha) H(x) dx\right)^{-1}, \tag{31}$$

where

$$g(x,\alpha) = \frac{3(\alpha+2)(1-\alpha)x^6 - 6(\alpha-1)^2 x^3}{[(\alpha+2)x^3 + 2(\alpha-1)]^2}. \tag{32}$$

Note that

$$g(x,\infty) = \frac{-3x^3}{x^3 + 2}, \tag{33}$$

$$g(x,0) = \frac{3}{2}\frac{x^3}{x^3 - 1}. \tag{34}$$

Thus, lower bound (31) yields a nonzero result for perfectly insulating spheres $\alpha = 0$ provided that $H(x)$ vanishes as $(x-1)^\beta$ at $x = 1$, where $\beta > 0$. This is contrast to conventional lower bounds such as the Hashin–Shtrikman lower bound, which, for $\alpha < 1$, is also generally given by (24) and always vanishes when $\alpha = 0$.

III. CALCULATION OF THE SECURITY-SPHERES BOUNDS

In this section we compute the security-spheres bounds on σ_e for two models: simple cubic and random arrays of spheres of radius a. We focus our attention on cases of infinite contrast ($\alpha = \infty$ or 0). Our results shall be compared to the well-known Hashin–Shtrikman (HS) bounds and to bounds very recently derived by Bruno.[9]

A. Simple-cubic-array results

Consider a situation in which the spheres are centered on a lattice of minimum spacing $d\lambda$. The nearest-neighbor distribution function is then given by

$$dH(x) = \delta(x - \lambda), \tag{35}$$

where $\delta(x)$ is a Dirac delta function. Thus, upper and lower bounds (23) and (31), respectively, become

$$\frac{\sigma_e}{\sigma_1} \leqslant 1 + \phi_2 f(\lambda,\alpha) \tag{36}$$

and

$$\frac{\sigma_e}{\sigma_1} \geqslant [1 + \phi_2 g(\lambda,\alpha)]^{-1}, \tag{37}$$

where $f(\lambda,\alpha)$ and $g(\lambda,\alpha)$ are given by (20) and (32), respectively. For a simple cubic array, the dimensionless distance λ is related to the sphere volume fraction by

$$\lambda^3 = \frac{\pi}{6\phi_2}. \tag{38}$$

Not surprisingly, both (36) and (37) are exact through the first order in ϕ_2.

1. Superconducting spheres

For the case of superconducting spheres ($\alpha = \infty$), the security-spheres bounds (36) and (37) yield

$$\frac{\sigma_e}{\sigma_1} \leqslant 1 + 3\phi_2 \frac{\lambda^3}{\lambda^3 - 1}, \tag{39}$$

$$\frac{\sigma_e}{\sigma_1} \geqslant \left(1 - 3\phi_2 \frac{\lambda^3}{\lambda^3 + 2}\right)^{-1}. \tag{40}$$

Note that the upper bound, unlike conventional upper bounds, becomes infinite only when the spheres touch (i.e., $\lambda = 1$), as exactly is the case. The HS bounds in this instance are, for $\phi_2 > 0$, given by

$$\frac{\sigma_e}{\sigma_1} \leqslant \infty, \tag{41}$$

$$\frac{\sigma_e}{\sigma_1} \geqslant \frac{1 + 2\phi_2}{1 - \phi_2}. \tag{42}$$

Thus, while the HS lower bound (42) is generally sharper than (40), the HS upper bound (41) is clearly generally weaker than the security-spheres upper bound (39). To explain the reasons for such behavior, it is useful to recall the composite-sphere assemblages that are realized by the HS bounds. The HS upper bound for $\alpha > 1$ corresponds to "composite" spheres consisting of a core of conductivity σ_1, surrounded by a concentric shell of conductivity, with the relative amount of each phase determined solely by the volume fraction ϕ_2. The composite spheres fill all space, implying a distribution in their size ranging to the infinitesimally small. The HS lower bound for $\alpha > 1$ corresponds to the same geometry, but with phase 1 interchanged with phase 2. Therefore, for $\phi_2 > 0$, the conducting phase corresponding to the HS upper bound is always connected and for $\alpha = \infty$ always percolates. The security-spheres upper bound (39), on the other hand, incorporates information that there must always be a security shell around each sphere and therefore remains finite unless the spheres touch. In contrast, the security-spheres trial field for the lower bound (40) provides a generally poor estimate of the energy exterior to the spheres relative to the HS lower-bound geometry. In summary, among the aforementioned two sets of bounds for conducting spheres ($\alpha \gg 1$), one should employ the security-spheres upper bound and the HS lower bound. In Fig. 1 we plot for $\alpha = \infty$ these bounds along with the exact solution for simple cubic arrays.[12]

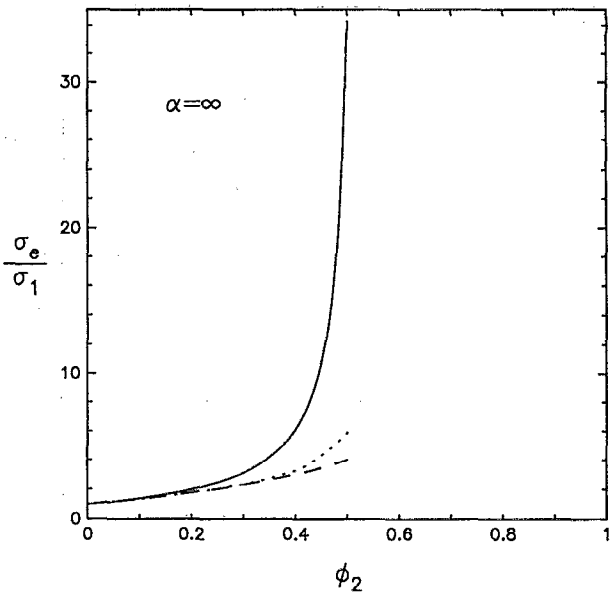

FIG. 1. The scaled effective conductivity σ_e/σ_1 for superconducting ($\alpha = \infty$) simple cubic arrays of spheres. Dashed line is the HS lower bound (Ref. 1), dotted line represents exact data (Ref. 12), and the solid line is the security-spheres upper bound (39).

2. Perfectly insulating spheres

In the instance of perfectly insulating spheres ($\alpha = 0$), the security-sphere bounds (36) and (37) give

$$\frac{\sigma_e}{\sigma_1} \leqslant 1 - 3\phi_2 \frac{\lambda^3}{2\lambda^3 + 1}, \tag{43}$$

$$\frac{\sigma_e}{\sigma_1} \geqslant \left(1 + 3\phi_2 \frac{\lambda^3}{2(\lambda^3 - 1)}\right)^{-1}. \tag{44}$$

Observe that the lower bound, unlike conventional lower bounds, vanishes only when the spheres touch (i.e., $\lambda = 1$). The HS bounds for $\alpha = 0$ and $\phi_2 > 0$ are given by

$$\frac{\sigma_e}{\sigma_1} \leqslant \frac{\phi_1}{1 + \phi_2/2}, \tag{45}$$

$$\frac{\sigma_e}{\sigma_1} \geqslant 0. \tag{46}$$

Although the HS upper bound (45) is generally better than (43), the HS lower bound vanishes in contrast to the security-spheres lower bound (44). The reasons for this behavior are similar to the explanations given above for the superconducting case and hence are not given here. Thus, among these bounds for insulating spheres ($\alpha \ll 1$), one should use the HS upper bound and the security spheres lower bound. In Fig. 2 we depict for $\alpha = 0$ these bounds along with the exact solution.[12]

Bruno[9] has very recently derived bounds on σ_e for particulate composites which are related to but not the same

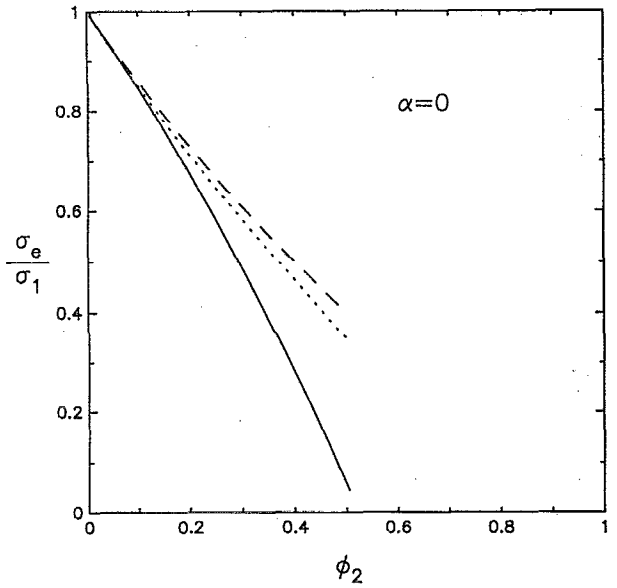

FIG. 2. The scaled effective conductivity σ_e/σ_1 for perfectly insulating ($\alpha = 0$) simple cubic arrays of spheres. Dashed line is the HS upper bound (Ref. 1), dotted represents exact data (Ref. 12), and the solid line is the security-spheres lower bound (44).

as the security-spheres bounds. Besides the security-spheres bounds, the former represents the only other bounds which remain nontrivial in the limit of infinite contrast. Bruno uses the elegant complex variable method to obtain bounds on σ_e which depend on the particle volume fraction ϕ_2, particle shapes, and a quantity q equal to the minimum, for all particles in the composite, of the ratio of the particle diameter to the sum of the diameter and the distance to the nearest neighbor. For a simple cubic lattice of equisized spheres, q is precisely equal to λ^{-1}. For random systems of identical spheres, the nearest-neighbor interparticles distances will vary (i.e., the system is generally not well spaced in the sense defined in the Introduction), and hence q for many such ensembles will not be a good descriptor of the microstructure. Bruno's upper bound, in the case of $\alpha \gg 1$, will be relatively sharp, provided that the microstructure is well described by a single parameter q (e.g., a lattice of spheres). The same bounds will not be sharp for microgeometries in which the spheres are not all "well spaced" (e.g., random systems in general). Bruno's lower bound for $\alpha > 1$ and upper bound for $\alpha < 1$ coincide with the corresponding HS bounds. Lower bounds for $\alpha > 1$ and upper bounds for $\alpha < 1$, which improve upon the corresponding HS bounds, have been computed for sphere distributions, however.[14] In other words, our main interest is in the improvement of conventional upper bounds for $\alpha \gg 1$ and conventional lower bounds for $\alpha \ll 1$.

In Table I we compare, for a simple cubic array, the security-spheres upper bound (40) with Bruno's corresponding result for superconducting particles ($\alpha = \infty$) and the security-spheres lower bound (44) with Bruno's corresponding bound for perfectly insulating particles ($\alpha = 0$). As indicated above, Bruno's bounds are sharper

TABLE I. Bounds on the scaled effective conductivity σ_e/σ_1 for simple cubic arrays in the superconducting ($\alpha = \infty$) and perfectly insulating ($\alpha = 0$) limits. S_U and B_U denote the security-spheres upper bound (39) and Bruno's upper bound, respectively. S_L and B_L denote the security-spheres lower bound (44) and Bruno's lower bound, respectively.

	$\alpha = \infty$		$\alpha = 0$	
ϕ_2	S_U	B_U	S_L	B_L
0.1	1.37	1.35	0.844	0.855
0.2	1.97	1.86	0.673	0.716
0.3	3.11	2.80	0.487	0.567
0.4	6.08	5.21	0.282	0.385
0.5	34.28	28.00	0.057	0.101

for this model. As shall be shown in the following subsection, this is often not the case for random arrays.

B. Random-array results

In order to evaluate the security-spheres bounds (23) and (31), one needs to have the nearest-neighbor distribution function $H(r)$ for random arrays of spheres. This was recently given by Torquato and co-workers[11] for the case of identical particles of diameter d and spheres volume fraction ϕ_2, and in dimensionless form is given by

$$dH(x;\phi_2) = \begin{cases} 0, & x < 1, \\ h(x;\phi_2), & x > 1, \end{cases} \tag{47}$$

where

$$h(x;\phi_2) = 24\phi_2(c_0 + c_1 x + c_2 x^2)\exp\{-\phi_2[8c_2(x^3-1) + 12c_1(x^2-1) + 24c_0(x-1)]\}, \tag{48}$$

$$c_0 = \frac{\phi_2^2}{2(1-\phi_2)^3},$$

$$c_1 = \frac{-\phi_2(3+\phi_2)}{2(1-\phi_2)^3},$$

$$c_2 = \frac{1+\phi_2}{(1-\phi_2)^3}. \tag{49}$$

Relation (47) has been tested against computer-simulation results[15] and was found to be very accurate up to about $\phi_2 = 0.6$, corresponding to a volume fraction near the random close-packing value. (The random close-packing volume fraction has been determined to range from $\phi_2 = 0.61$ to 0.66.[16]) Substitution of (47) into (23) in the limit $\alpha \to \infty$ yields the trivial upper bound $\sigma_e/\sigma_1 \leqslant \infty$ since $H(x) \neq 0$ at $x = 1$. Similarly, the combination of (47) and (31) gives the trivial lower bound $\sigma_e/\sigma_1 \geqslant 0$ in the limit $\alpha \to 0$.

In order to get nontrivial bounds in the extreme-contrast cases, we coat each sphere of conductivity σ_2 and diameter d with a thin layer of matrix material of conductivity σ_1. Let d_0 be the diameter of these composite spheres at the actual inclusion volume fraction $\phi_2 = \rho\pi d^3/6$. As far as the structure is concerned, we are actually interested in random hard spheres of diameter $d_0 \geqslant d$ and volume fraction

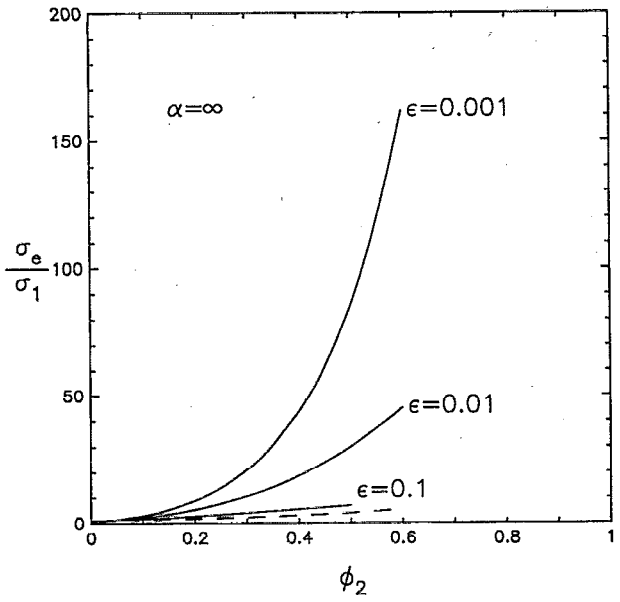

FIG. 3. Bounds on the scaled effective conductivity σ_e/σ_1 for superconducting ($\alpha=\infty$) random arrays of spheres characterized by a nearest-neighbor distribution function given by (51) for several values of the dimensionless coating thickness ϵ. Dashed line is the HS lower bound (Ref. 1), and the solid lines are the security-spheres upper bound (23).

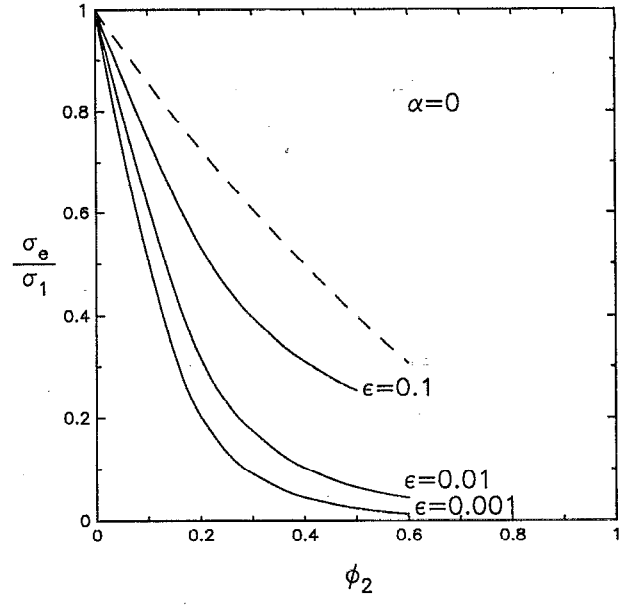

FIG. 4. Bounds on the scaled effective conductivity σ_e/σ_1 for perfectly insulating ($\alpha=0$) random arrays of spheres characterized by a nearest-neighbor distribution function given by (51) for several values of the dimensionless coating thickness ϵ. Dashed line is the HS upper bound (Ref. 1), and the solid lines are the security-spheres lower bound (31).

$$\hat{\phi}_2=\frac{\rho\pi d_0^3}{6}=\left(\frac{d_0}{d}\right)^3\phi_2. \tag{50}$$

Thus, the dimensionless nearest neighbor distribution function we require is given by

$$dH\left(\frac{d}{d_0}x;\hat{\phi}_2\right)=\begin{cases}0, & x<\dfrac{d_0}{d},\\ \dfrac{d}{d_0}h\left(\dfrac{d}{d_0}x;\hat{\phi}_2\right), & x>\dfrac{d_0}{d}.\end{cases} \tag{51}$$

In Fig. 3 we plot the security-spheres upper bound (23) for superconducting random arrays ($\alpha=\infty$) using (51) for several values of the dimensionless coating thickness ϵ defined by

$$\epsilon=\frac{d_0-d}{d}. \tag{52}$$

Included in the figure is the HS lower bound. The HS upper bound is infinite and hence does not appear. As ϵ is made smaller, the upper bound becomes larger at fixed volume fraction ϕ_2, as expected. Note that the upper and lower bounds shown in the figure can be quite tight for small to moderate values of ϕ_2. For $\epsilon=0.1$, $\phi_2>0.5$ is not possible.

Figure 4 depicts the security-spheres lower bound (31) for perfectly insulating random arrays ($\alpha=0$) using (51) for several values of ϵ. The figure includes the HS upper bound. The HS lower bound vanishes identically. Not surprisingly, as ϵ is made smaller, the lower bound decreases at fixed ϕ_2. Again, the upper and lower bounds can be stringent for small to moderate ϕ_2.

Tables II and III compare for random arrays our upper bounds when $\alpha=\infty$ and lower bounds when $\alpha=0$, respectively, to the corresponding Bruno bounds for several values of ϵ. For reasons mentioned earlier, our bounds are generally significantly better than Bruno's bounds. For $\epsilon=0.001$ and $\alpha=\infty$, the security-spheres upper bound is, on average, an order of magnitude smaller than Bruno's upper bound for the range $0\leqslant\phi_2\leqslant0.4$. The corresponding security-spheres lower bound for insulating spheres shows similar improvement over the Bruno lower bound. For $\epsilon=0.01$, the security-spheres results are generally sharper than Bruno's results, but the improvement is not a great as for the smaller value of the coating thickness ($\epsilon=0.001$). Finally, at the largest coating thickness considered ($\epsilon=0.1$), Bruno's bounds are sharper than the security-

TABLE II. Upper bounds on the scaled effective conductivity σ_e/σ_1 for superconducting ($\alpha=\infty$) random arrays of spheres characterized by a nearest-neighbor distribution function given by (51). ϵ is the dimensionless coating thickness defined by (52). ϕ_2 is the actual inclusion volume fraction. S_U and B_U denote the security-spheres upper bound (23) and Bruno's upper bound, respectively. For $\epsilon=0.1$, $\phi_2=0.6$ represents a physically unattainable volume fraction.

	$\epsilon=0.001$		$\epsilon=0.01$		$\epsilon=0.1$	
ϕ_2	S_U	B_U	S_U	B_U	S_U	B_U
0.1	2.937	70.1	2.26	8.08	1.67	1.88
0.2	8.800	144.2	5.32	15.7	2.73	2.84
0.3	20.91	223.8	10.6	23.8	4.03	3.88
0.4	43.67	309.5	18.6	32.6	5.44	5.02
0.5	85.32	402.1	30.1	42.2	6.85	6.27
0.6	161.5	502.5	45.2	52.5	–	–

TABLE III. Lower bounds on the scaled effective conductivity σ_e/σ_1 for perfectly insulating random arrays of spheres characterized by a nearest-neighbor distribution function given by (51). ϵ is the dimensionless coating thickness defined by (52). ϕ_2 is the actual inclusion volume fraction. S_L and B_L denote the security-spheres lower bound (31) and Bruno's lower bound, respectively. For $\epsilon = 0.1$, $\phi_2 = 0.6$ represents a physically unattainable volume fraction.

	$\epsilon = 0.001$		$\epsilon = 0.01$		$\epsilon = 0.1$	
ϕ_2	S_L	B_L	S_L	B_L	S_L	B_L
0.1	0.508	0.0528	0.616	0.345	0.748	0.772
0.2	0.204	0.0252	0.318	0.197	0.535	0.610
0.3	0.091	0.0156	0.174	0.131	0.397	0.488
0.4	0.045	0.0108	0.103	0.094	0.310	0.393
0.5	0.024	0.0079	0.065	0.070	0.255	0.317
0.6	0.012	0.0059	0.044	0.053	–	–

spheres bounds in almost all instances, albeit only slightly better. This last observation is not that surprising since the system becomes increasingly well spaced and hence less "random" as ϵ becomes larger.

IV. CONCLUSIONS

We have derived security-spheres bounds on the effective conductivity σ_e for distributions of spheres which do not necessarily become trivial in the infinite-contrast limits, unlike conventional bounds such as the Hashin–Shtrikman bounds. Bruno[9] has very recently derived bounds on σ_e which are related to the security-spheres bounds. These are the first set of bounds that can treat the difficult infinite-contrast limits and therefore must be regarded as the first generation of such bounds. Bruno's bounds are useful in that they depend only upon the parameter q and the volume fraction, yielding relatively sharp bounds when the particles are well spaced. On the other hand, since they are so general, the bounds can be somewhat weak when the microstructure is not well described by a single parameter (e.g., random arrays). By construction, the security-spheres bounds are relatively weak when the particles are well spaced, but can be comparatively sharp [as the result of incorporating higher-order information via the nearest-neighbor distribution function $H(r)$] for random arrays. For random arrays, the security-spheres bounds are more general then Bruno's bounds in that they not only depend on ϵ, but on $H(r)$, which varies from ensemble to ensemble. Thus, we suggest that a future study combine the aforementioned advantageous features for each of these bounds to derive even better bounds.

ACKNOWLEDGMENTS

The authors thank O. P. Bruno for supplying an early draft of his manuscript and for valuable discussions. S. T. gratefully acknowledges the partial support of the Office of Basic Energy Sciences, U.S. Department of Energy under Grant No. DE-FG05-86ER13482 and the Air Force of Scientific Research under Grant No. 90-0090. J. R. acknowledges the support of the Technion V. P. R.

APPENDIX A: SECURITY-SPHERE BOUNDARY-VALUE PROBLEM WITH CONTINUITY OF POTENTIAL

Consider a composite sphere consisting of a sphere of conductivity σ_2 and radius a surrounded by a concentric "security" shell of conductivity σ_1 and outer radius b. This composite sphere is immersed in an infinite medium of conductivity σ_1 in which the applied field is $\mathbf{E}_0$. Let $T(\mathbf{x})$ be the potential and $\mathbf{E}(\mathbf{x}) = -\nabla T(\mathbf{x})$. We seek the solution to the following boundary-value problem:

$$\Delta T = 0, \quad \text{for} \quad 0 \leqslant r \leqslant b, \tag{A1}$$

$$T \text{ finite at } r = 0, \tag{A2}$$

$$T \text{ and } J_n \text{ continuous at } r = a, \tag{A3}$$

$$T = -|\mathbf{E}_0| b \cos\theta \text{ at } r = b. \tag{A4}$$

Here, r is the radial distance measured with respect to the sphere center, θ is the corresponding polar angle, and J_n is the normal flux.

This boundary-value problem is easily solved using separation of variables with the result that

$$\mathbf{E} = \begin{cases} \dfrac{3\lambda^3 \mathbf{E}_0}{(\alpha+2)\lambda^3 + (1-\alpha)}, & r < a, \\ \dfrac{(\alpha+2)\lambda^3 \mathbf{E}_0}{(\alpha+2)\lambda^3 + (1-\alpha)} + \dfrac{(\alpha-1)a^3\lambda^3}{(\alpha+2)\lambda^3 + (1-\alpha)} \\ \quad \times \dfrac{[3(\mathbf{E}_0 \cdot \hat{\mathbf{r}})\,\hat{\mathbf{r}} - \mathbf{E}_0]}{r^3}, & a \leqslant r \leqslant b. \end{cases} \tag{A5}$$

Here, $\hat{\mathbf{r}} = \mathbf{r}/|\mathbf{r}|$ is the radial unit vector, $\lambda = b/a$, and $\alpha = \sigma_2/\sigma_1$.

APPENDIX B: SECURITY-SPHERE BOUNDARY-VALUE PROBLEM WITH CONTINUITY OF NORMAL FLUX

We now reconsider the problem of Appendix A with the boundary condition (A4) replaced by

$$\frac{\partial T}{\partial r} = -|\mathbf{E}_0| \cos\theta, \quad \text{at } r = b. \tag{B1}$$

All other boundary conditions are the same. The solution to this problem is given by

$$\mathbf{E} = \begin{cases} \dfrac{3\lambda^3 \mathbf{E}_0}{(\alpha+2)\lambda^3 + 2(\alpha-1)}, & r < a, \\ \dfrac{(\alpha+2)\lambda^3 \mathbf{E}_0}{(\alpha+2)\lambda^3 + 2(\alpha-1)} + \dfrac{(\alpha-1)a^3\lambda^3}{(\alpha+2)\lambda^3 + 2(\alpha-1)} \\ \quad \times \dfrac{[3(\mathbf{E}_0 \cdot \hat{\mathbf{r}})\,\hat{\mathbf{r}} - \mathbf{E}_0]}{r^3}, & a \leqslant r \leqslant b. \end{cases} \tag{B2}$$

[1] Z. Hashin and S. Shtrikman, J. Appl. Phys. **33**, 3125 (1962).
[2] M. Beran, Nuovo Cimento **38**, 771 (1965).
[3] G. W. Milton, J. Appl. Phys. **52**, 5294 (1981).
[4] S. Torquato, J. Appl. Phys. **58**, 3790 (1980).
[5] I. C. Kim and S. Torquato, J. Appl. Phys. **68**, 3892 (1990); I. C. Kim and S. Torquato, J. Appl. Phys. **69**, 2280 (1991).
[6] J. B. Keller, L. Rubenfeld, and J. Molyneux, J. Fluid Mech. **30**, 97 (1967).

[7] J. Rubinstein and S. Torquato, J. Chem. Phys. **88**, 6372 (1988); S. Torquato and J. Rubinstein, J. Chem. Phys. **90**, 1644 (1989).
[8] J. Rubinstein and S. Torquato, J. Fluid Mech. **206**, 25 (1989).
[9] O. P. Bruno (unpublished).
[10] S. Torquato, J. Chem. Phys. **84**, 6345 (1986).
[11] S. Torquato, B. Lu, and J. Rubinstein, J. Phys. A **23**, L103 (1990); S. Torquato, B. Lu, and J. R. Rubinstein, Phys. Rev. A **41**, 2059 (1990).
[12] R. C. McPhedran and D. R. McKenzie, Proc. R. Soc. London A **359**, 45 (1978).
[13] D. J. Bergman, Phys. Rep. **43**, 378 (1978).
[14] See, for example, S. Torquato and F. Lado, Phys. Rev. B **33**, 6248 (1986); S. Torquato, Appl. Mech. Rev. **44**, 37 (1991), and references therein.
[15] S. Torquato and S. B. Lee, Physica A **164**, 347 (1990).
[16] J. G. Berryman, Phys. Rev. A **27**, 1053 (1983).